IEEE Access
Multidisciplinary : Rapid Review : Open Access Journal

Received April 24, 2017, accepted May 13, 2017, date of publication May 23, 2017, date of current version July 3, 2017.

Digital Object Identifier 10.1109/ACCESS.2017.2707060

Source Location Identification of Distribution-Level Electric Network Frequency Signals at Multiple Geographic Scales

WENXUAN YAO[1], (Student Member, IEEE), JIECHENG ZHAO[1], (Student Member, IEEE), MICAH J. TILL[1], (Student Member, IEEE), SHUTANG YOU[1], (Student Member, IEEE), YONG LIU[1], (Member, IEEE), YI CUI[1], (Student Member, IEEE), AND YILU LIU[1,2], (Fellow, IEEE)

[1]Department of Electrical Engineering and Computer Science, The University of Tennessee, Knoxville, TN 37996, USA
[2]Oak Ridge National Laboratory, Oak Ridge, TN 37831, USA

Corresponding author: Wenxuan Yao (wyao3@utk.edu)

This work was supported in part by the Engineering Research Center Shared Facilities through the Engineering Research Center Program of the National Science Foundation and DOE under NSF Award EEC-1041877 and in part by the CURENT Industry Partnership Program.

ABSTRACT The distribution-level electric network frequency (ENF) extracted from an electric power signal is a promising forensic tool for multimedia recording authentication. Local characteristics in ENF signals recorded in different locations act as environmental signatures, which can be potentially used as a fingerprint for location identification. In this paper, a reference database is established for distribution-level ENF using FNET/GridEye system. An ENF identification method that combines a wavelet-based signature extraction and feedforward artificial neural network-based machine learning is presented to identify the location of unsourced ENF signals without relying on the availability of concurrent signals. Experiments are performed to validate the effectiveness of the proposed method using ambient frequency measurements at multiple geographic scales. Identification accuracy is presented, and the factors that affect identification performance are discussed.

INDEX TERMS Distribution-level, ENF signal, frequency measurement, signature extraction, location identification.

I. INTRODUCTION

The electric network frequency (ENF), which typically fluctuates around its a nominal value (50 or 60 Hz) and faithfully reflects the balance between generation and load, has becoming an emerging forensic tool for recorded media authentication [1]. The ENF criterion was first proposed by Grigoras [2] and since then copious research has been conducted, mainly focusing on techniques for ENF extraction from multimedia recordings or the use of ENF as a signature to ascertain the time, location and authenticity of recordings [3]–[7].

However, there are significant fundamental questions remaining, prominently: what are the limitations of ENF location identification? Can the ENF signal from a given location be regarded as unique in order to verify the place a recoding was taken? The answers to these two question could potentially pave the way for the usage of ENF-based applications and provide direction to future research for recording authentication.

It is well known that power grid frequency in different interconnections is determined by the overall balance between generation and load [8]. Thus, the ENF signals recorded across different interconnections can be distinguished using a feather extraction method and machine learning system [9]. For the ENF within an interconnection, most existing research assumes that the signals across an interconnected power grid are identical [9]–[11]. However, in a real power system, it is likely that there are some minor variations in ENF signals recorded at different locations. A power system disturbance such as a generator trip may have an effect on the whole grid which propogates with measurable time coefficients [12]. In [13], [14], the location estimation within an interconnection is realized based on correlation coefficient (CC) on different locations. However, it needs availability of concurrent ENF signals to obtain the CC. It is known that in the United States Eastern Interconnection (EI), these frequency changes propagate throughout the grid at a speed of approximately 500 miles per second [15]. Moreover, the various electromechanical propagation speeds for the effects of changes in local loads to other locations mean that some slight variation or transient differences may be uniquely reflected in local ENF signals. Furthermore, due to nonlinear load and recurrent local disturbance, environmental noises such as fluctuation and variation of ENF may result some long-term signatures in the ambient ENF data in different locations. It is hypothesized that these signatures, if successfully extracted, might be potentially used for ENF location identification within an interconnection, which will significantly broaden the scope of ENF related applications. Following this, the objective of this paper is to develop a machine learning implementation to identify the characteristics of ENF from different locations and classify ENF signals by their geographic source. To verify this hypothesis, this paper explores the possibility of retrieving signatures from ENF signal using real power grid frequency measurements recorded within a single interconnection.

In this paper, a reference database is first established for distribution-level ENF using the FNET/GridEye system. Second, this paper proposes a new approach which combines signature extraction and machine learning. An L-level Daubechies wavelet is used to remove the common component from an ENF signal and a Fourier transform is used to extract the local signatures. To determine the source location of the ENF, a feed-forward artificial neural network (F-ANN) is applied to the extracted signature [16], [17]. These experiments use FNET/GridEye frequency measurements from the EI at multiple geographic scales (500 miles, 200 miles, and 2 miles) to evaluate identification performance. The accuracy of ENF location identification is given and the factors which influence identification accuracy are discussed. The outcomes of this work are beneficial for authentication of digital multimedia and preventing cyber attacks on critical infrastructure, e.g., power systems, by detecting if real data have been tampered with or wholly replaced by fake data.

The rest of this paper is organized as follows: Section II introduces the establishment of an ENF reference database. Section III presents the proposed approach for signature extraction and source location identification. Section IV examines the cases studies for ENF location identification using frequency measurements from the FNET/Grid system and discusses the factors which influence the results. Finally, conclusions and future work are given in Section V.

II. ENF REFERENCE DATABASE

Establishing an ENF reference database is a prerequisite for the application of multimedia recording authentication using an ENF criterion [18]–[20]. To apply the multimedia recording authentication, an ENF signal embedded in a multimedia recording is extracted and then matched against a pre-established ENF reference database. For the multimedia recording ENF extraction, either time or frequency domain methods, such as the zero-crossing method [2], [5], spectrogram and subspace-based signal processing techniques [4], [19], [21], wavelet or short-time Fourier transform (STFT) [3], [11], are used.

Phasor measurement units (PMUs), invented in the 1980s and installed in high-voltage transmission-level substations, are able to provide Global Positioning System (GPS) time-synchronized frequency measurements, which can be used as a data source for the ENF database [7], [22], [23]. However, frequency measurements at the transmission level do not observe the local distribution-level characteristics, e.g., small load changes, leading to inapplicability of the ENF identification on a granular geographic scale.

Originally developed in 2003, the Frequency Monitoring Network (FNET/GridEye) system is a wide-area phasor measurement system at the distribution-level [24]–[26]. Precise frequency measurements (at an accuracy of 0.0005 Hz) obtained by Frequency Disturbance Recorders (FDRs), members of the PMU familly, are time-stamped using GPS synchronization [27]–[29]. A photo of a generation-II FDR is shown in Fig. 1. As of November 2016, more than 250 FDRs have been deployed across North America as depicted in Fig. 2 [30].

FIGURE 1. Photo of a generation-II frequency disturbance recorder.

The ENF reference database can be established using the data aggregated on FNET/GridEye servers. The architecture of the ENF database, as illustrated in Fig. 3, mainly consists of three components: frequency sensors, Internet-based communication infrastructure, and data servers. FDRs act as sensors recording the instantaneous ENF every 0.1 seconds and transmitting them to a data center at the University of Tennessee, Knoxville(UTK) for storage and analysis. The FNET/Grideye system provides data storage and application functions (e.g., disturbance detection, oscillation detection, post-disturbance analysis, and web services) [15], [24], [25]. Internet-based communication infrastructure provides communication channels between

FIGURE 2. Map of FDR deployment in North America.

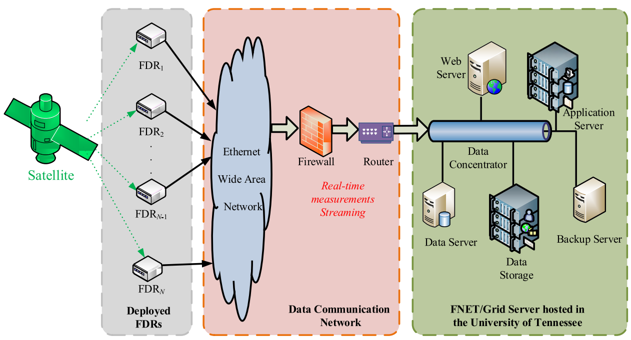

FIGURE 3. The framework of FNET/GridEye system.

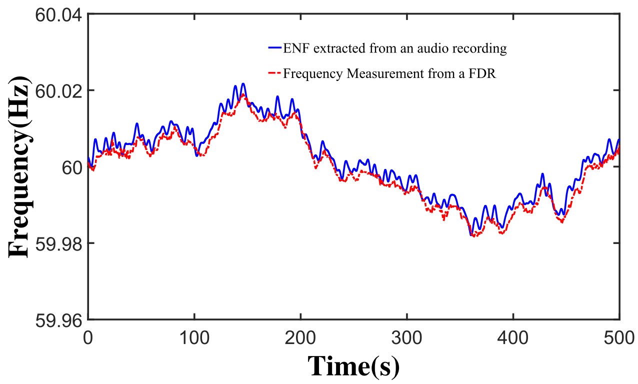

FIGURE 4. Plot of FDR measurement and ENF extracted from an audio recording.

FDRs and FNET/GridEye servers. Earlier studies show that frequency measurements collected via the FNET/GridEye system are able to match the frequency extracted from digital recordings using the iterative oscillation error correction method and STFT [3], [11], [31], [32]. Fig. 4 demonstrates the effectiveness of the FNET/GridEye system as an ENF reference database.

III. METHODOLOGY

A. SIGNATURE EXTRACTION FROM ENF SIGNAL

Due to hardware failure, e.g., GPS signal loss, spoofing, or network interruption [30], [33]–[35], FDRs frequently suffer from invalid and missing data. To avoid bad training of the recognition model using pre-collected frequency measurements from the database, the continuity and validity of data are checked prior to signature extraction from ENF signal. Since each measurement is synchronized with a GPS time index, a discontinuous index implies missing data. In order to adequately train the F-ANN for ENF identification in this study, a minimum length of 15-minute of uninterrupted frequency data (9000 continuous data points) are required. If sufficient data is not available for a given unit in a certain time window, data from that window belonging to that unit is excluded. Frequency measurement spikes are identified using a median filter. Spikes that exceed a preset threshold are replaced by values from median filter results. The advantage of this spike identification method from [36] is that it only eliminates isolated spikes while keeping all other raw data intact, preserving as much detailed frequency information as possible.

Since local frequency affects are of interest, it is essential to remove the common frequency component from each signal in the interconnection in order to extract local signatures from ENF signals. Fig. 5 shows concurrent frequency measurements recorded from three FDRs at different locations in the EI. It can be observed that all three frequency curves are highly correlated with a common component. Variations from this component can be seen more clearly in the callout window.

One approach to remove the common component is to subtract the median frequency for all units in the interconnection from the original signal. The median frequency, which can be obtained using the median filter method, is chosen to approximate grid frequency due to its robustness with a large number of units running concurrently [37]. The median frequency method is straightforward and effective in removal of the common component.

However, the performance of the median frequency based extraction method is significantly influenced by the number of FDRs with available data. In the case where there is only one or two FDRs identified with available data, median frequency cannot precisely represent the common component. Therefore, in this paper, an L-level Daubechies wavelet-based extraction method is applied instead, where each level provides an approximation to the original signal and the detailed variations at a specific level of resolution. Assuming the ENF signals $\mathrm{ENF}_1 \ldots \mathrm{ENF}_n$ are absolutely and square integrable, the wavelet transform of $\mathrm{ENF}_n(t)$ can be expressed as

$$Wf(v,\lambda) = \frac{1}{\sqrt{v}} \int_{-\infty}^{+\infty} \mathrm{ENF}_n(t)\Psi^*\left(\frac{t-\lambda}{v}\right) dt \qquad (1)$$

where v and λ are defined as the dilation and time-translation parameters respectively. The mother function Ψ^* is a Daubechies wavelet satisfying admissibility condition [38].

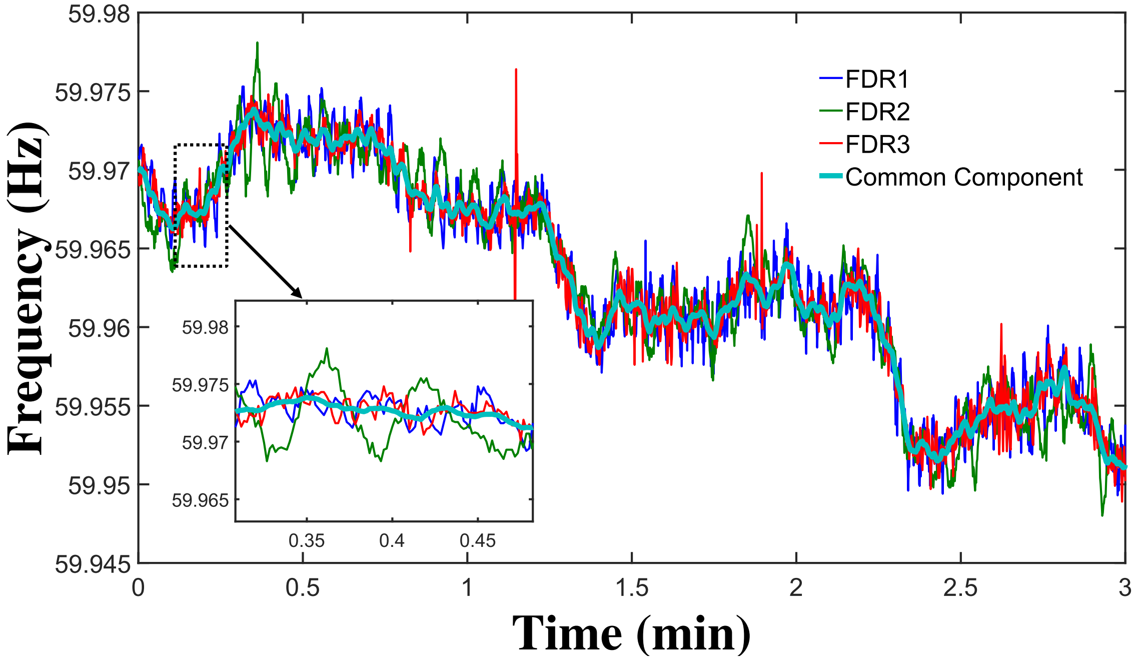

FIGURE 5. The plot of raw frequency measurements recorded on difference locations in EI.

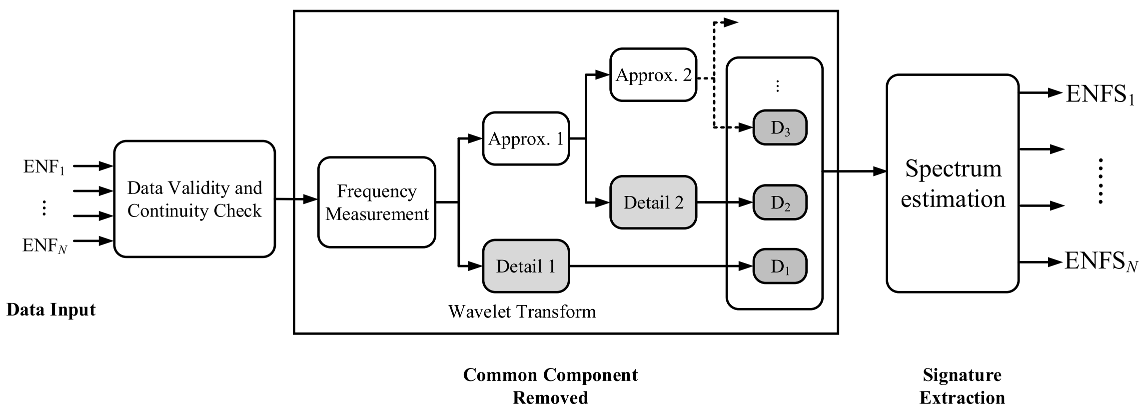

FIGURE 6. Flowchart of the signature extraction from raw ENF signal.

As illustrated in Fig. 6 the lower time variance of the lower time-frequency band (the approximation) is considered to be the common component of the frequency measurements and the variances of the high-pass band (e.g., Detail 1 and Detail 2) can potentially be used for local signatures extraction. Although the wavelet-based method introduces greater computational complexity than the median frequency method, it is more flexible and can obtain local signatures without relying on the availability of concurrent ENF signals.

Fig. 7 shows the signatures extracted from three FDRs using the wavelet-based method of Detail 1. It can been seen that the signatures from ENF signal are chaotic and stochastic in the time domain. It is assumed that the local signatures may have specific patterns in the frequency domain. Therefore, the fast Fourier transform with a window length of 600 data points (1 minute of data) and a 10 second moving window is performed to obtain the input spectrum for F-ANN as illustrated in Fig. 8. It can be observed that each of the signatures has a distinct spectral distribution attributed to local factors that can be used as input samples when training the F-ANN for source location identification.

B. ENF LOCATION IDENTIFICATION

The spectrum data $ENFS_1 \ldots ENFS_n$ of frequency measurements in the database recorded from different locations and time periods is used to train the three-layer F-ANN. The structure of the F-ANN is illustrated in Fig. 9. An FDR outputs 600 frequency measurements per minute. The input vector is the absolute value of 1 minute ENF spectrum. The length of the input vector is 300 since the FFT spectrum is symmetrical.

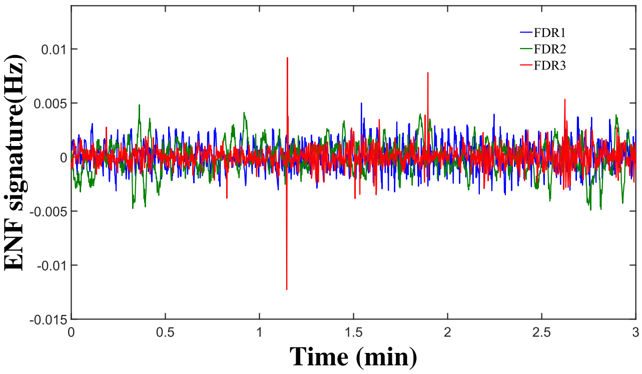

FIGURE 7. Signature extraction from ENF signal using wavelet transform.

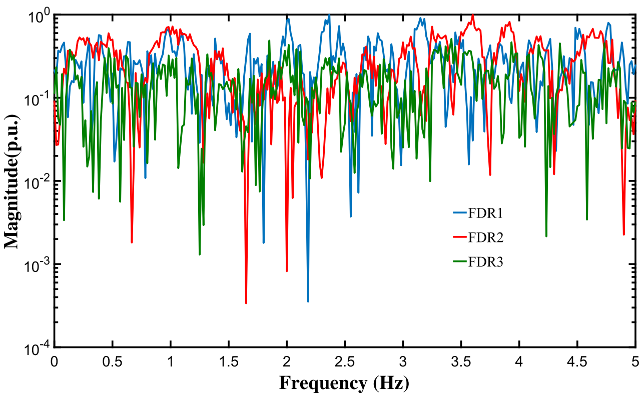

FIGURE 8. Spectrum distribution of extracted signature from raw ENF signal.

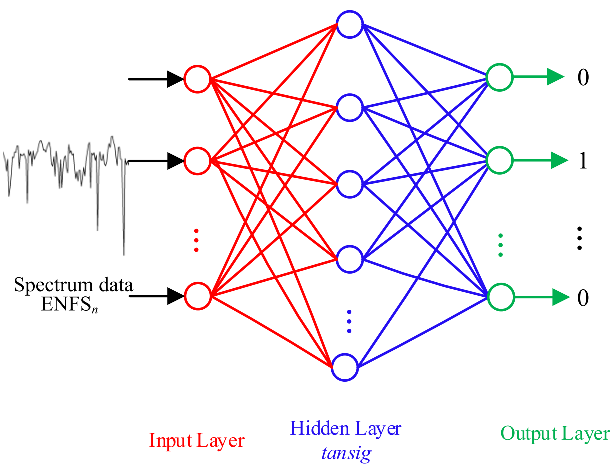

FIGURE 9. Structure of the F-ANN.

The target vector is the column vector of a size equal to the number of FDR locations. Each target vector has "0"s in all rows except one. The position of the unique "1" element in each column indicates the location of the corresponding input vector. For example, a "1" in the nth row of a target vector indicates that the corresponding input vector originated from a unit with index n. The transfer function *tansig* for the hidden layer is defined as

$$tansig(x) = \frac{2}{1 + e^{-2x}} - 1 \tag{2}$$

In the final layer, a *softmax* function is used to normalize the output to (0,1] while preserving ordering. This function is defined as

$$softmax(z_n) = \frac{e^{y_n}}{\sum_{n=1}^{N} e^{y_n}} \quad for\ n = 1, \cdots, N \tag{3}$$

where y_n is the output from the hidden layer and N is the number of locations. The purpose of the *softmax* function is to approximate a unitary target vector $z_n \subseteq (0, 1]$. The most likely location of the input vector is determined at the maximum value of the output vector. For the training process, these input vectors are provided alongside target vectors. Training vectors are randomly assigned to training, validation, or test sets, satisfying 70% for training, 15% for validation, and 15% for testing. Once the F-ANN is trained, it will be used to identify the location of ENF signals from an unknown source recorded outside the time window covered by training data as illustrated in Fig. 10.

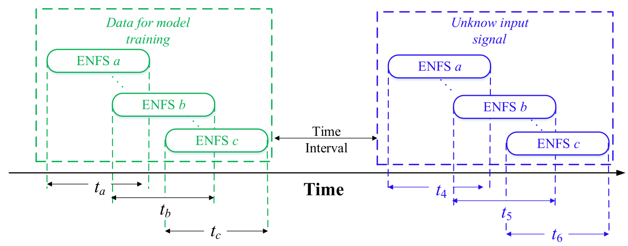

FIGURE 10. Illustration of location identification of extracted signatures from ENF signals.

IV. PERFORMANCE EVALUATION

Taking advantage of the widespread deployment of FDRs, experiments are carried out to test the performance of the proposed approach for location identification. Frequency measurement data from are obtained from the FNET/Grideye. Historical data from each of locations is used to train the F-ANN and then an signal of unknown origin (from one of the training unit locations for the purpose of this analysis) is identified using the F-ANN. Three geographic scales, Case I (500 miles), Case II (200 miles) and Case III (2 miles), are tested. Five FDRs are randomly selected for each case. For case I, FDRs in difference EI states (Missouri, Tennessee, South Carolina, West Virginia, and Florida) with a minimum distance of approximate 500 miles between any two units, are selected as mapped in Fig. 11. For Case II, FDRs deployed in states of Alabama, Tennessee, Kentucky and Georgia with a minimum distance of approximate 200 miles between units are selected and mapped in Fig. 11. For the Case III, five locations in the city of Knoxville, Tennessee, are selected as shown in Fig. 12.

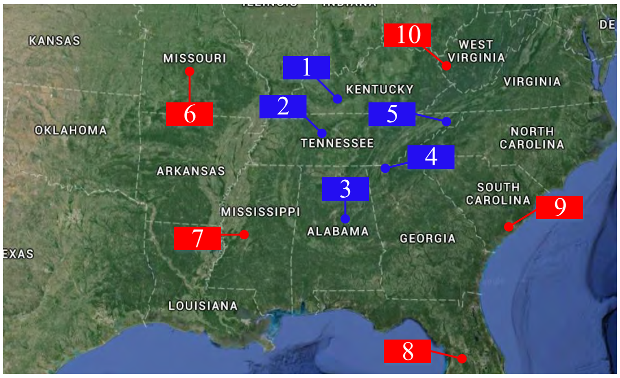

FIGURE 11. Map of FDR locations for Case I and Case II. Red labels: Case I. Blue labels: Case II.

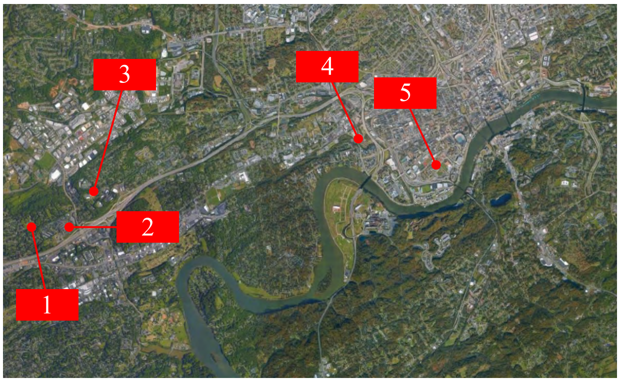

FIGURE 12. Map of FDR locations for Case III.

A. MODEL TRAINING

A 3-layer F-ANN is trained using historical data by the back-propagation algorithm for location identification of given signals. The number of neurons greatly influences the identification accuracy and training time. After some trial and error, it was found in this study that the optimally number of neurons in the hidden layer is 30. Further increasing the number of neurons will not substantially improve accuracy, but does lead to longer training times. As discussed in Section III, the FFT spectrum of the extracted signature serves as an input vector for training. Each of these input vectors is assigned a corresponding target vector, which defines the location where the signal originated. In each case, the target vector is a five element column vector. For fair comparison, a 30-minute data set is used for each unit with a sliding window length of 10 points. Therefore, a total of 2.7×10^6 data points were fed to the F-ANN during the training process.

B. RESULTS OF ENF LOCATION IDENTIFICATION

The objective of the trained F-ANN is to determine the location of a signal of unknown origin from one of the locations providing historical training data. For any input signature vector, the F-ANN will return an output vector. The column index of the output vector with the highest value indicates the corresponding location to be the most likely source of the signal. To evaluate the performance of the F-ANN, the overall identification accuracy is defined as

$$Accuracy = \frac{I_{correct}}{I_{total}} \times 100\% \tag{4}$$

where $I_{correct}$ represents the number of vectors that are correctly identified and I_{total} is the total number of vectors tested.

The identification accuracy for each case under different time intervals is listed in Table 1. It can be seen that Case I has the highest accuracy. The location of the a given signal can be identified at matching rate larger than 90% given a 6-month time interval. The accuracy is as large as 80.4% given a 12-month time interval between the signal of unknown origin and training data in Case I. The confusion matrices of identification accuracy for Case I with time intervals 1 month and 12 months are shown in Tables 2 and 3, respectively. For each table, the labels of the columns represent the actual location of the signals tested while the labels of the rows denote the location predicted by the F-ANN. The entries in the highlighted diagonals show the correct identification accuracy for each location. The accuracies are high, ranging from 97.23% to 98.82% (1 month) and 78.82% to 82.67% (12 months) for all locations, which demonstrates the effectiveness of the trained F-ANN for location identification.

TABLE 1. Accuracy for FDR location identification.

Case	Time Interval	Identification Accuracy(%)
I	1 day	99.8
	1 week	99.3
	1 month	98.2
	6 months	90.1
	12 months	80.4
II	1 day	95.6
	1 week	99.3
	1 month	91.5
	6 months	50.2
	12 months	34.4
III	1 day	42.6
	1 week	35.3

TABLE 2. Confusion Matrix for Case I with a 1-month Time Interval.

The location of tested FDRs		MI	TN	SC	WV	FL
Estimated location	MI	98.23	0.62	0.17	0.97	0.60
	TN	0.29	97.57	0.59	0.11	0.53
	SC	0.71	1.12	98.15	0.14	0.31
	WV	0.20	0.05	0.68	98.51	0.24
	FL	0.57	0.64	0.41	0.27	98.32

TABLE 3. Confusion Matrix for Case I with a 12-month Time Interval.

The location of tested FDRs		MI	TN	SC	WV	FL
Estimated location	MI	80.42	3.21	4.51	5.78	6.24
	TN	5.15	82.67	3.59	5.26	3.45
	SC	4.56	5.21	81.56	4.99	7.21
	WV	6.12	2.97	1.98	79.12	4.28
	FL	3.75	5.94	8.36	4.85	78.82

There are three potential reasons for the phenomenon that the accuracy varies in different time. First, the local load may change with time (different seasons in a year). Therefore, the environmental noises, which contributes some portions in the local signatures, may be different when local loads are changed, e.g., switching on/off a cooling/heating system. As a result, in some occasions the environmental noise is very strong while environmental noises become weaker or even disappeared in some other occasions. Second, in a real power system, large disturbances may happen and overwhelm long-term environmental noises. The impact of this kind of disturbances is that the local signatures of ENF signal is still there but hard to be extracted. Third, for our machine learning system, only 1-minute data points are used for identification test. It will be possible that the identified signatures is not covered in the 1-minute data set. The accuracy of the identification are influenced by whether testing data have recorded the sufficient local and extractable signatures.

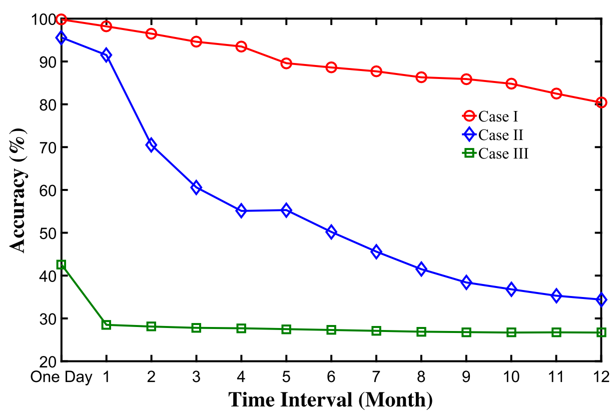

FIGURE 13. Identification accuracy versus the time interval used.

As illustrated in Fig. 13, the accuracy of Case I is slightly reduced with the increased time intervals. This drop may be caused by the local load change with time. Therefore, to obtain high identification accuracy, the latest available data are preferred for the machine learning. In Case II, identification accuracy with a time interval of 1 month (91.5%) is slightly lower than in Case I (98.2%). Moreover, the rate of this decrease is greater than in Case I. Case III has a smallest geographic scale and considerably lower identification accuracy (below 50%) than Cases I and II. Therefore, it can be generally concluded from these results that location identification of a signal with a relatively large geographic scale leads to better performance than identification with a small geographic scale.

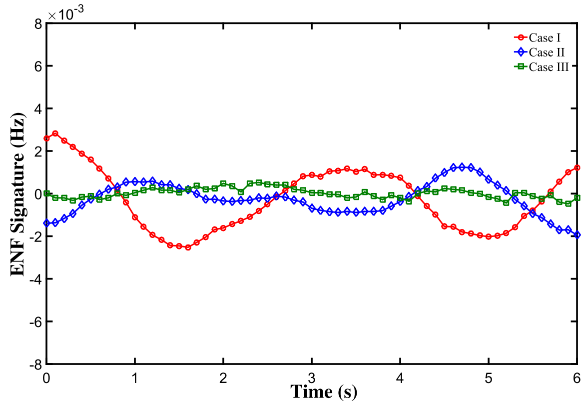

FIGURE 14. Comparison of extracted signatures from ENF signals.

C. DISCUSSION

To explore accuracy differences across geographic scales, the wavelet-extracted signatures are compared in Fig. 14. A smaller magnitude of extracted signatures is observed as the geographic scale decreases. For Case I, the amplitude of the extracted signature is as large as 3.12×10^{-3} Hz compared with 5.21×10^{-4} Hz for Case III.

As the signature is smaller given shorter distances, the signal may be heavily overwhelmed at the distribution-level by measurement uncertainty or noise. Therefore the wavelet approach cannot effectively extract any distinct features from ENF signals, leading to the low identification accuracy of F-ANN. For Case III, the amplitude of the signature is close to the FDR frequency measurement resolution of 5.0×10^{-4} Hz.

To examine the correlation between extracted signatures in each case, the normalized cross-correlation of two ENF signals can be expressed as

$$\rho_{k,l} = \frac{\sum_{n=1}^{N} f_k(n) f_l(n)}{\sqrt{\sum_{n=1}^{N} f_k(n)^2 \cdot \sum_{n=1}^{N} f_l(n)^2}} \tag{5}$$

where N is the length of each of two signals and $f_l(n)$ is the ENF signal at time n and location l. The probability distributions of normalized cross-correlation for each case is shown in Fig. 15. From Fig. 15, the extracted signature with a relatively small geographic scale has a considerable high value of normalized cross-correlation distribution, which indicated a high similarity in ENF signals. This might cause the ENF difficulty to be differentiated. The mean normalized cross-correlations for each case are listed in Table 4. It can be seen from Table 4 that the value of cross-correlation of Case III (0.8484) is approximately 3 times larger than the value in Case I (0.2872). When the geographic scale is not large

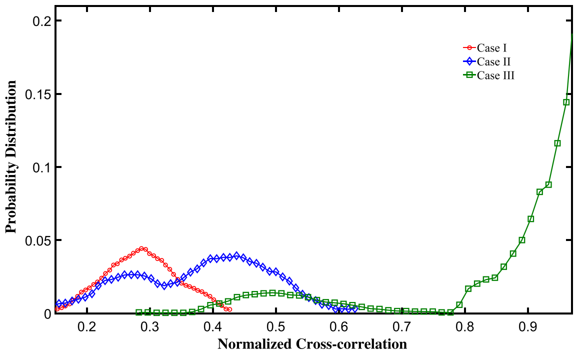

FIGURE 15. The probability distribution of normalized cross-correlation.

TABLE 4. Comparison of Normalized Cross-Correlation of Extracted Signature.

Case	Normalized Cross-correlation
I	0.2872
II	0.4112
III	0.8484

enough, the signatures are relatively attenuated and highly correlated. As a result, it is possible that the "true" signature is mostly subsumed by measurement uncertainty and noise, masking the identification references and leading to mistakes in location estimation. Therefore, to identify the ENF location at a small geographic scale, measurement device accuracy must significantly improve.

V. CONCLUSIONS AND FUTURE WORK

In this paper, a machine learning-based method is developed to identify the location of an ENF signal of unknown origin without concurrent information. First, an ENF reference database is established from FNET/GridEye measurement. Second, an L-level Daubechies wavelet is used for signature extraction from ENF signal and a pre-trained F-ANN to identify the location from which the signal originated.

Three case studies at multiple geographic scales are carried out using frequency data from the FNET/GridEye system to evaluate the performance and applicability of the proposed method. It is found that the accuracy of this method is dependent upon the geographic scales of the input ENF signal. For a large geographic scale (500 miles), accuracy of more than 90% and 80% can be achieved using 6 and 12 month time intervals, respectively. This verifies the effectiveness of the proposed method on large geographic scale location identification. For a small geographic scale, identification accuracy is low. To address why accuracy drops significantly with a smaller geographic scale, the signatures extracted from each case are compared. It is found that the signatures over a small geographic scale have high values of normalized cross-correlation. As a result, the true local signatures are likely to be subsumed by measurement uncertainty and noise, thus negatively impacting source location identification.

Since ENF signals carry strong potential as location stamps, future work will focus on improving the accuracy of identification with small geographic scales. At the current stage, only frequency measurement signals are used for identification. The next step is to exploit FNET/Grideyes synchronized voltage angle and amplitude measurements as supplementary information. Moreover, increasing the sampling and reporting rate may be another possible approach to increase accuracy.

REFERENCES

[1] G. Hua, J. Goh, and V. L. L. Thing, "A dynamic matching algorithm for audio timestamp identification using the ENF criterion," *IEEE Trans. Inf. Forensics Security*, vol. 9, no. 7, pp. 1045–1055, Jul. 2014.

[2] C. Grigoras, "Applications of ENF criterion in forensic audio, video, computer and telecommunication analysis," *Forensic Sci. Int.*, vol. 167, nos. 2–3, pp. 136–145, Apr. 2007. [Online]. Available: http://www.sciencedirect.com/science/article/pii/S0379073806004312

[3] Y. Liu, Z. Yuan, P. N. Markham, R. W. Conners, and Y. Liu, "Application of power system frequency for digital audio authentication," *IEEE Trans. Power Del.*, vol. 27, no. 4, pp. 1820–1828, Oct. 2012.

[4] R. Garg, A. L. Varna, A. Hajj-Ahmad, and M. Wu, "'Seeing' ENF: Power-signature-based timestamp for digital multimedia via optical sensing and signal processing," *IEEE Trans. Inf. Forensics Security*, vol. 8, no. 9, pp. 1417–1432, Sep. 2013.

[5] C. Grigoras, "Applications of ENF analysis in forensic authentication of digital audio and video recordings," *J. Audio Eng. Soc.*, vol. 57, no. 9, pp. 643–661, 2009. [Online]. Available: http://www.aes.org/e-lib/browse.cfm?elib=14835

[6] D. P. N. Rodríguez, J. A. Apolinário, and L. W. P. Biscainho, "Audio authenticity: Detecting ENF discontinuity with high precision phase analysis," *IEEE Trans. Inf. Forensics Security*, vol. 5, no. 3, pp. 534–543, Sep. 2010.

[7] M. M. Elmesalawy and M. M. Eissa, "New forensic ENF reference database for media recording authentication based on harmony search technique using GIS and wide area frequency measurements," *IEEE Trans. Inf. Forensics Security*, vol. 9, no. 4, pp. 633–644, Apr. 2014.

[8] H. Ma and H. Li, "Analysis of frequency dynamics in power grid: A Bayesian structure learning approach," *IEEE Trans. Smart Grid*, vol. 4, no. 1, pp. 457–466, Mar. 2013.

[9] A. Hajj-Ahmad, R. Garg, and M. Wu, "ENF-based region-of-recording identification for media signals," *IEEE Trans. Inf. Forensics Security*, vol. 10, no. 6, pp. 1125–1136, Jun. 2015.

[10] O. Ojowu, J. Karlsson, J. Li and Y. Liu, "ENF extraction from digital recordings using adaptive techniques and frequency tracking," *IEEE Trans. Inf. Forensics Security*, vol. 7, no. 4, pp. 1330–1338, Aug. 2012.

[11] L. Fu, P. N. Markham, R. W. Conners, and Y. Liu, "An improved discrete Fourier transform-based algorithm for electric network frequency extraction," *IEEE Trans. Inf. Forensics Security*, vol. 8, no. 7, pp. 1173–1181, Jul. 2013.

[12] G. Zheng, Y. Liu, and G. Radman, "Wide area frequency based generation trip event location estimation," in *Proc. IEEE Power Energy Soc. General Meeting*, Jul. 2012, pp. 1–6.

[13] R. Garg, A. Hajj-Ahmad, and M. Wu, "Geo-location estimation from electrical network frequency signals," in *Proc. ICASSP*, 2013, pp. 2862–2866.

[14] A. Hajj-Ahmad, R. Garg, and M. Wu, "Instantaneous frequency estimation and localization for ENF signals," in *Proc. Asia–Pacific Signal Inf. Process. Assoc. Annu. Summit Conf.*, Dec. 2012, pp. 1–10.

[15] Y. Liu *et al.*, "Wide-area-measurement system development at the distribution level: An FNET/Grideye example," *IEEE Trans. Power Del.*, vol. 31, no. 2, pp. 721–731, Apr. 2016.

[16] C. J. Mantas, "A generic fuzzy aggregation operator: Rules extraction from and insertion into artificial neural networks," *Soft Comput.*, vol. 12, no. 5, pp. 493–514, 2008. [Online]. Available: http://dx.doi.org/10.1007/s00500-007-0221-8

[17] S. P. Fard and Z. Zainuddin, "Almost everywhere approximation capabilities of double Mellin approximate identity neural networks," *Soft Comput.*, vol. 20, no. 11, pp. 4439–4447, 2016. [Online]. Available: http://dx.doi.org/10.1007/s00500-015-1753-y

[18] A. J. Cooper, "The electric network frequency (ENF) as an aid to authenticating forensic digital audio recordings—An automated approach," in *Proc. Audio Eng. Soc. Conf., 33rd Int. Conf., Audio Forensics-Theory Pract.*, Jun. 2008, pp. 1–3. [Online]. Available: http://www.aes.org/e-lib/browse.cfm?elib=14411

[19] M. Kajstura, A. Trawinska, and J. Hebenstreit, "Application of the electrical network frequency (ENF) criterion: A case of a digital recording," *Forensic Sci. Int.*, vol. 155, nos. 2–3, pp. 165–171, 2005. [Online]. Available: http://www.sciencedirect.com/science/article/pii/S0379073804007662

[20] E. B. Brixen, "Further investigation into the ENF criterion for forensic authentication," in *Proc. Audio Eng. Soc. Conv. 123*, Oct. 2007, pp. 1–6. [Online]. Available: http://www.aes.org/e-lib/browse.cfm?elib=14333

[21] E. B. Brixen, "Techniques for the authentication of digital audio recordings," in *Proc. Audio Eng. Soc. Conv. 122*, May 2007, pp. 1–8. [Online]. Available: http://www.aes.org/e-lib/browse.cfm?elib=13999

[22] A. G. Phadke, "Synchronized phasor measurements in power systems," *IEEE Comput. Appl. Power*, vol. 6, no. 2, pp. 10–15, Apr. 1993.

[23] W. Yao *et al.*, "A novel method for phasor measurement unit sampling time error compensation," *IEEE Trans. Smart Grid*, to be published.

[24] Y. Zhang *et al.*, "Wide-area frequency monitoring network (FNET) architecture and applications," *IEEE Trans. Smart Grid*, vol. 1, no. 2, pp. 159–167, Sep. 2010.

[25] Y. Liu *et al.*, "Recent developments of FNET/GridEye—A situational awareness tool for smart grid," *CSEE J. Power Energy Syst.*, vol. 2, no. 3, pp. 19–27, Sep. 2016.

[26] Z. Zhong *et al.*, "Power system frequency monitoring network (FNET) implementation," *IEEE Trans. Power Syst.*, vol. 20, no. 4, pp. 1914–1921, Nov. 2005.

[27] J. Chai, J. Zhao, W. Yao, J. Guo, and Y. Liu, "Application of wide area power system measurement for digital authentication," in *Proc. IEEE/PES Transmiss. Distrib. Conf. Expo. (T&D)*, May 2016, pp. 1–5.

[28] J. Chai *et al.*, "Wide-area measurement data analytics using FNET/Grideye: A review," in *Proc. Power Syst. Comput. Conf. (PSCC)*, Jun. 2016, pp. 1–6.

[29] Y. C. Zhang, W. Yao, J. Culliss, G. Zhang, Z. Teng, and Y. Liu, "Electrical field based wireless devices for contactless power gird phasor measurement," in *Proc. IEEE PES General Meeting/Conf. Expo.*, Jul. 2014, pp. 1–5.

[30] W. Yao *et al.*, "Impact of GPS signal loss and its mitigation in power system synchronized measurement devices," *IEEE Trans. Smart Grid*, to be published.

[31] Y. Liu, C. Yao, C. Sun, and Y. Liu, "The authentication of digital audio recordings using power system frequency," *IEEE Potentials*, vol. 33, no. 2, pp. 39–42, Mar. 2014.

[32] Y. Liu, Z. Yuan, P. N. Markham, R. W. Conners, and Y. Liu, "Wide-area frequency as a criterion for digital audio recording authentication," in *Proc. IEEE Power Energy Soc. General Meeting*, Jul. 2011, pp. 1–7.

[33] L. Zhan, Y. Liu, W. Yao, J. Zhao, and Y. Liu, "Utilization of chip-scale atomic clock for synchrophasor measurements," *IEEE Trans. Power Del.*, vol. 31, no. 5, pp. 2299–2300, Oct. 2016.

[34] P. Zhang and K. W. Chan, "Reliability evaluation of phasor measurement unit using Monte Carlo dynamic fault tree method," *IEEE Trans. Smart Grid*, vol. 3, no. 3, pp. 1235–1243, Sep. 2012.

[35] Y. Fan, Z. Zhang, M. Trinkle, A. D. Dimitrovski, J. B. Song, and H. Li, "A cross-layer defense mechanism against GPS spoofing attacks on PMUs in smart grids," *IEEE Trans. Smart Grid*, vol. 6, no. 6, pp. 2659–2668, Nov. 2015.

[36] W. Li, J. Tang, J. Ma, and Y. Liu, "Online detection of start time and location for hypocenter in North America power grid," *IEEE Trans. Smart Grid*, vol. 1, no. 3, pp. 253–260, Dec. 2010.

[37] Y. Liu, Z. Yuan, P. N. Markham, R. W. Conners, and Y. Liu, "Power grid frequency data conditioning using robust statistics and B-spline functions," in *Proc. IEEE Power Energy Soc. General Meeting*, Jul. 2012, pp. 1–6.

[38] K. L. V. Iyer, X. Lu, Y. Usama, V. Ramakrishnan, and N. C. Kar, "A twofold Daubechies-wavelet-based module for fault detection and voltage regulation in SEIGs for distributed wind power generation," *IEEE Trans. Ind. Electron.*, vol. 60, no. 4, pp. 1638–1651, Apr. 2013.

WENXUAN YAO (S'14) received the B.S. and Ph.D. degrees in electrical engineering from Hunan University, Changsha, China, in 2011 and 2017, respectively. He is currently pursuing the Ph.D. degree with the Department of Electrical Engineering and Computer Science, The University of Tennessee, Knoxville, TN, USA. His current research interests include wide-area power system monitoring, synchrophasor measurement applications, embedded system development, power quality diagnosis, and big data analysis for the power system.

JIECHENG ZHAO (S'15) received the B.S. degree in automatic control from Huazhong University of Science and Technology, Wuhan, China, in 2008, and the Ph.D. degree in radio physics from the University of Chinese Academy of Sciences, Beijing, China, in 2013. He is currently pursuing the Ph.D. degree in electrical engineering with The University of Tennessee, Knoxville, TN, USA. His current research interests include power system monitoring.

MICAH J. TILL (S'13) received the B.S.E.E. degree from Tennessee Technological University, Cookeville, TN, USA, in 2011, and the M.S.E.E. from The University of Tennessee, Knoxville, TN, USA, in 2015, where he is currently pursuing the Ph.D. degree with the Department of Electrical Engineering and Computer Science.

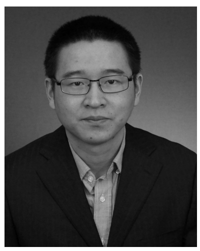

SHUTANG YOU (S'13) received the B.S. and M.S. degrees in electrical engineeringfrom Xi'an Jiaotong University, China, in 2011 and 2014, respectively. He is currently pursuing the Ph.D. degree with the Power IT Lab, The University of Tennessee, Knoxville, TN, USA. His current research interests include power grid dynamics modeling and monitoring, system operation simulation, and expansion planning, as well as the application of signal processing techniques in power grids.

YONG LIU (S'10–M'15) received the B.S. and M.S. degrees of electrical engineering from Shandong University in 2007 and 2010, respectively, and the Ph.D. degree from The University of Tennessee, Knoxville, TN, USA, in 2013. He is currently a Research Assistant Professor with the Department of Electrical Engineering and Computer Science, The University of Tennessee, Knoxville. He is a member of DOE/NSF co funded engineering research center, CURENT. His current research interests include power system wide-area measurement, renewable energy integration, and power system dynamic modeling and analysis.

YI CUI (S'12) received the B.Sc. and M.Sc. degrees in electrical engineering from Southwest Jiaotong University, Chengdu, China, in 2009 and 2012, respectively, and the Ph.D. degree in electrical engineering from The University of Queensland, Brisbane, Australia, in 2016. He is currently a Postdoctoral Research Fellow with the Department of Electrical Engineering and Computer Science, The University of Tennessee, Knoxville, TN, USA. His current research interests include wide-area monitoring and control, measurement-based small signal stability, condition assessment, and fault diagnosis for power transformers.

YILU LIU (S'88–M'89–SM'99–F'04) received the B.S. degree from Xian Jiaotong University and the M.S. and Ph.D. degrees from The Ohio State University, Columbus, OH, USA, in 1986 and 1989. She was a Professor with Virginia Tech. She is a member of the U.S. National Academy of Engineering. She is currently the Governor's Chair with The University of Tennessee, Knoxville, TN, USA, and the Oak Ridge National Laboratory. She led the effort to create the North American power grid Frequency Monitoring Network with Virginia Tech, which is now operated at UTK and ORNL as GridEye. Her current research interests include power system wide-area monitoring and control, large interconnection-level dynamic simulations, electromagnetic transient analysis, and power transformer modeling and diagnosis.